Progress In Electromagnetics Research Letters, Vol. 42, 141–154, 2013

CALCULATION OF THE CURRENTS GENERATED IN DENTAL TISSUES BY THE APPLICATION OF AN EXTERNAL ELECTRIC FIELD

Leonardo Sandrolini*

Department of Electrical, Electronic, and Information Engineering, University of Bologna, Viale del Risorgimento 2, Bologna I-40136, Italy

Abstract—The application of an external electric field has been shown to enhance the impregnation of resin monomers used in restorative dentistry. Further to experimental investigations that have related the migration of monomers to their electrical properties, additional insight into the conduction mechanism within the tooth can be gained by numerical modelling of the current conduction through the tooth. This paper presents the development of a three-dimensional realistic voxel model of a human tooth from a data set of digital images and the computation of the currents in the dental tissues by means of a low-frequency numerical code (scalar potential finite difference). Results for the electric potential and current density magnitude in various cross sections of the tooth model are presented for an applied 10 V dc voltage between the electrodes.

1. INTRODUCTION

Contemporary restorative dentistry techniques are based on the mechanical application of dentin adhesives to tooth structures by means of a sponge or a brush. In the last years a novel restorative technique has been proposed which makes use of an electric field to enhance resin monomers impregnation of the dentin [1]. By applying a dc voltage between an application sponge filled with an adhesive and the etched tooth substrate a constant electric flow during the adhesive application is created. An insight into the mechanisms of monomer migration under the application of an electric field can be found in [2], where the electrical properties of the resin monomers are measured and it is shown that the electrophoretic effect is enhanced

Received 9 July 2013, Accepted 28 August 2013, Scheduled 4 September 2013

* Corresponding author: Leonardo Sandrolini (leonardo.sandrolini@unibo.it).

by high values of electrical conductivity. These findings may be used to quantify the effect of electric currents on impregnation of monomers with a modelling approach.

The characterization of the conduction through the tooth may be useful also for other applications in dental practice, such as the endodontic treatment. This application is a method of root canal therapy in which pulp is removed and the root canal is cleaned and sealed; for a successful treatment, a precise determination of the root canal length of the tooth is required [3]. Electronic methods have been proposed which determine the root canal length from the measurement of the impedance between a metal file inserted in the root canal and an outer electrode placed on the oral mucosa. Modelling the current conduction through the human tooth allows the impedance of the tooth to be calculated and related to the electrical parameters of the tooth. The modelling can be done with either an equivalent circuit or a numerical simulation. With the latter, insight into the current conduction through the tooth may be added. In [3], the numerical modelling and computation of impedance exploit the finite element analysis. Notwithstanding, the model used in [3] for the numerical simulations is not realistic and consists in a solid obtained by boolean operations on simple geometrical forms. It can then be acknowledged the need of a simulation tool for the assessment of the electric field and current density in the dental tissues due to an applied external dc voltage.

In this paper, the implementation of a numerical method for the calculation of the currents generated in dental tissues by the application of an external electric field is presented. A three-dimensional realistic model of the tooth, obtained from a dataset of digital photographes, is developed. The calculation of the currents is carried out numerically using the scalar potential finite difference (SPFD) method [4, 5]. Results for the electric potential and current density in various sections of the model are presented. The paper is organized as follows. In Section 2, the mathematical formulation of the problem is presented, and the computational method is described. In Section 3 the procedure to build a numerical model for the tooth is outlined. The results of the analysis of the current conduction in the tooth are presented in Section 4.

2. MATHEMATICAL FORMULATION

The calculation of the current in the dental tissues was carried out with the SPFD method, which is described in detail in [4, 5]. In its general formulation, the SPFD method incorporates the applied magnetic field

source as a vector potential term in the electric field; the electric field equation is then transformed into a scalar potential form and solved using finite differences. The method has been successfully applied to the calculation of induced currents in a number of problems concerning health effects of low-frequency electromagnetic fields on humans [6–8]. A feature of the method consists in confining the computational domain to the body model only, thus saving computational memory and time. The SPFD method assumes a quasi-static description of the electromagnetic field and can be applied to an isolated conducting body; under this assumption, Stevenson's method [9] can be applied to expand each of the incident, scattered and interior electromagnetic fields near the conductor in a power series involving the parameter $-jk_0$, where k_0 is the wavenumber in vacuum.

The application of the SPFD to the problem of calculating the current generated in the dental tissues involves two modifications of the general formulation, as in [10–12]. In this case, the excitation is provided by a couple of electrodes which simulate the application sponge and a current collector (ground electrode), respectively. The two electrodes are located on the surface of the tooth. The application of a dc voltage between the electrodes yields a mixed Dirichlet-Neumann problem, which has a determinate solution. The electric field inside the tooth can be written in terms of the electric scalar potential as

$$\mathbf{E}(\mathbf{r}) = -\nabla V(\mathbf{r}). \tag{1}$$

The conservation of the zeroth-order current density

$$\nabla \cdot \mathbf{J}(\mathbf{r}) = 0$$

requires that the potential satisfies the differential equation

$$\nabla \cdot [\sigma(\mathbf{r}) \nabla V(\mathbf{r})] = 0 \tag{2}$$

at any point inside the conducting body. At any point of the surface of the isolated conducting body, the boundary condition is

$$\hat{n}(\mathbf{r}) \cdot [\sigma(\mathbf{r}) \nabla V(\mathbf{r})] = 0 \tag{3}$$

where $\hat{n}(\mathbf{r})$ is the unit normal to the isolated conducting body surface (outward oriented). At each point of an electrode a known voltage is specified and the boundary condition is

$$V(\mathbf{r}) = V_e \tag{4}$$

where V_e is the constant static limit of the specified potential.

The numerical implementation of the SPFD method requires the three-dimensional computational domain (e.g., the conducting body) to be discretized into a set of elementary parallelepipeds or voxels;

within each voxel the electrical properties of the material are assumed constant. The electric potentials are defined at the vertices of the voxels, and the electric field is defined by set of discrete vectors on the voxel edges; the magnitude of the electric field is defined at the voxel centre by averaging the three sets of four parallel edge electric field components.

For each interior point of the tooth, the application of the divergence theorem to an imaginary voxel centred on that point allows Equation (2) to be approximated using finite differences as

$$\left(\sum_{h=1}^{6} S_h\right) \cdot V_0 - \sum_{h=1}^{6} (S_h \cdot V_h) = 0 \tag{5}$$

where V_0 is the electric potential at the voxel centre; V_h and $S_h = \bar{\sigma_h} a_h / l_h$, with $h = 1, \ldots, 6$ are the electric potential of one of the six vertices and the edge conductance of one of the six edges connected to it, respectively; a_h and l_h are the area of the voxel face normal to edge h and the length of the edge h, respectively; $\bar{\sigma_h}$ is the average electrical conductivity of the four voxels sharing edge h in common. Collecting Equations (5), (3) and (4) written for each vertex of each conducting voxel of the model yields an heptadiagonal system of equations

$$(\mathbf{N} - \mathbf{E})\,\mathbf{Y} = \mathbf{V} \tag{6}$$

where $\mathbf{Y}$ is the vector of unknown potentials, $\mathbf{V}$ the vector of specified potentials at the surface source electrodes, $\mathbf{N}$ a diagonal matrix whose elements are the sum of the edge conductances connected to the corresponding node, and $\mathbf{E}$ a symmetric matrix with at most six off-diagonal elements per row or column, whose elements are the conductances between adjacent vertices. This system is preconditioned and then solved with an iterative method such as GMRES (generalized minimum residual method). In a Cartesian coordinate system, once the potentials at the vertices of the model $\mathbf{Y}$ are found, for each voxel the electric field magnitude can be calculated from the three Cartesian components E_x, E_y and E_z as

$$E = \sqrt{E_x^2 + E_y^2 + E_z^2}. \tag{7}$$

For example, as Figure 1 shows, the component of the electric field in the x-direction of the generic voxel (i, j, k) belonging to the kth layer of the model can be found as

$$E_x = \frac{1}{4} \sum_{m=1}^{4} \frac{\triangle V_{x,m}}{l_{x,m}} \tag{8}$$

where $\triangle V_{x,m}$ is the difference of electric potential between two vertices of one of the four edges in the x-direction and $l_{x,m}$ the length of one

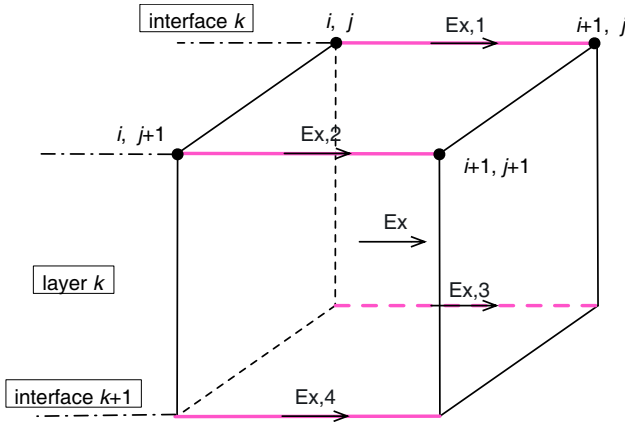

Figure 1. Electric field components in the x-direction for a generic voxel.

of the four edges in the x-direction. In turn, from Equation (7) the current density magnitude can be obtained

$$J = \sigma E. \tag{9}$$

The SPFD method described above was implemented in Matlab^{TM}. The development of a tooth voxel model used for the calculation of the currents generated in the dental tissues by the application of an external field is described in the next Section.

3. THREE-DIMENSIONAL TOOTH MODELLING

3.1. Development of Three-dimensional Tooth Model

A three-dimensional realistic voxel model of a human tooth was developed from a data set of scanned photographic images [13]. The tooth, a longitudinal section of which is shown in Figure 2, is a second premolar of a 33-years-old male. The data set consists of 806 digital 16-bit greyscale images with a 30 µm resolution in .raw format, each corresponding to a transversal cross-section (slice) of the tooth of 348×310 pixels (see Figure 3). In the three-dimensional model of the tooth, each pixel corresponds to a volume element (voxel) with an height of 30 µm; the total number of voxels representing the tooth is then $348 \times 310 \times 806 = 86,951,280$. Despite the tooth tissues are only three (enamel, dentin and pulp), each pixel has an intensity (i.e., shade of grey) ranging from 0 to about 7000. Thus, the huge number of voxels in combination with the large number of pixel intensities would make

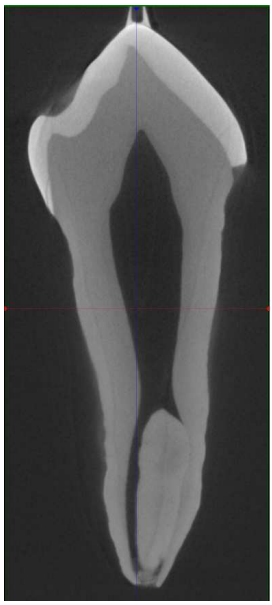

Figure 2. Longitudinal section of the tooth as imported by MicroView.

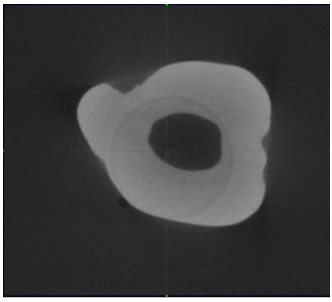

Figure 3. Digital image of a cross section of the tooth.

the model extremely computationally demanding for many simulation softwares, as each different intensity is interpreted as a different material. To overcome these problems, two actions were taken. On one side, the original data set of digital images was downsampled by a factor of 4, thus reducing the resolution of the model to 120 μm; on the other, the digital images of the data set were imported with the open source software MicroView and exported to DICOM (Digital Imaging and Communications in Medicine) format; each DICOM

image was then imported by Mathematica^{TM} and processed in order to associate the shades of grey to four different materials only (the three tooth tissues plus the background). A refinement procedure was implemented to remove anomalies in the digital images. Actually, in view of the numerical simulations, a fifth material (which represents the gum) was added to embed the tooth model in a number of sections. For this reason in Table 1, which presents the indices and electrical conductivities of the tooth tissues used in the numerical simulations, the gum does not present an intensity value. The electrical properties of the tooth tissues are not easily found in literature, and therefore the electrical conductivity is defined in a scale of tens: highest electrical conductivity for the pulp, lowest for the enamel and intermediate for dentin and gum. Some of these values are in agreement with those in [3]. The processed images were then collected in a three-dimensional array and saved to disk in .raw and .mat formats for later processing with either commercial electromagnetic simulation softwares or Matlab^{TM}, respectively. Matlab^{TM} was chosen to implement the SPFD method for its capability of handling large matrixes and vectors.

Table 1. Reference values and electrical conductivities of the tooth tissues.

Tissue	Index	Intensity	Electrical conductivity (S/m)
Background	0	0–2500	0
Dentin	1	2501–5100	10^{-3}
Enamel	2	5101–7000	10^{-5}
Pulp	3	0–2500	1
Gum	4	-	10^{-1}

3.2. Electrode Modelling

To model the contact electrodes across which the voltage is applied to the tooth, two rectangles were defined; the former represents the handset in contact with the etched tooth substrate and lies on a x-y plane perpendicular to the longitudinal axis (z-axis) of the model, the latter the current collector in contact with the gum and lies in a y-z plane of the model. Figure 4 shows a longitudinal section of the developed tooth model (same as of Figure 2) with the contact electrodes in position.

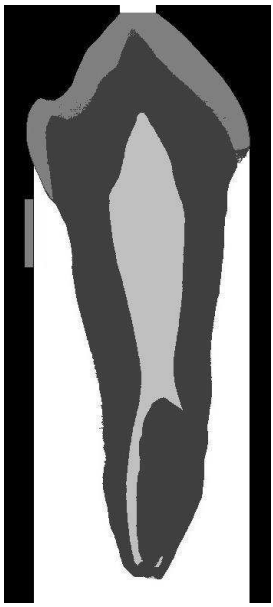

Figure 4. Longitudinal section of the developed three-dimensional model of the tooth with the contact electrodes. The white region represents the gum.

4. RESULTS

As described in the previous section, the heavy computational burden in terms of memory and time due to the huge number of voxels of the three-dimensional tooth model was alleviated by downsampling the original data set of digital images by a factor of 4, thus obtaining a three-dimensional model with $87 \times 78 \times 199 = 1,350,414$ voxels. Despite each voxel in the downsampled model has increased its volume of a factor of 4^3 with respect to the voxels of the original model, the increased resolution of 120 µm can still be acceptable to obtain significant information on the current density. Two electrodes were introduced in the model; the one representing the handset has 5×6 voxel faces and is located in a x-y plane on top of the tooth model (in contact with the enamel), the other representing the current collector (ground electrode) has 30×30 voxel faces and is in a y-z plane in contact with the gum in proximity of the enamel. The indicative positions of the electrodes are shown in Figure 4. A dc voltage of 10 V was applied between the electrodes. No restorative material was introduced in the model and thus the results obtained serve as

preliminary information in gaining an insight into the conduction mechanisms. The potential matrix system of Equation (6) consisted of 781,314 unknowns and was filled in 7.47 hours on a pc with a 2.67 GHz Intel core i7 CPU and 4 GB of RAM. The system was solved with GMRES in 10.3 minutes on the same machine. In the following, the results of the simulations carried out with the SPFD code are presented.

4.1. Electric Potential

The electric potential calculated in the tooth is shown in Figure 5 with reference to nine cross sections transversal to the tooth at various distances from the electrode with applied 10 V potential. As it can be expected, the potential decreases as the distance from the top electrode increases; it can be noticed that the decrease is indeed rapid, at a distance of 0.36 mm from the electrode, the maximum value for the electric potential in the tooth tissues (enamel) is already less than 7 V. The cross sections (b)–(d) in Figure 5 contain enamel and dentin tissues only; it can be noticed that the highest potential values, that are initially found in the external regions of the tooth (enamel), are found also in the interior region (dentin) as the distance increases. The potential values range from tens to few hundreds mV. The cross sections (e)–(g) in Figure 5 are at the height of the current collector electrode, whose potential is set to 0 V; the cross sections (e) and (f) contain all three tissues of the tooth, whereas the cross section (g) contains dentin and pulp only. The electric potential in the pulp region is of the order of the mV. The electric potential in the pulp starts then to decrease proceeding down the tooth, as Figures 5(h), (i) show; the values of the potential are anyway very small, in the order of tenths of mV.

4.2. Current Density

The current density magnitude calculated in the tooth is shown in Figure 6 with reference to nine transversal cross-sections at various distances from the electrode with applied 10 V potential. The cross section (a) of Figure 6 is the closest to the top electrode; as it can be expected, it shows high magnitude values for the current density, up to about 14 mA/m^2 in proximity to the electrode. With increasing distance from the electrode (cross sections (b)–(d) in Figure 6) the highest values of current density magnitude are in the interior region of the tooth (dentin), and at a distance of 3.84 mm the highest value is about 2 mA/m^2. In the cross sections (e) and (f) that contain all three tissues of the tooth and are at the height of the current collector

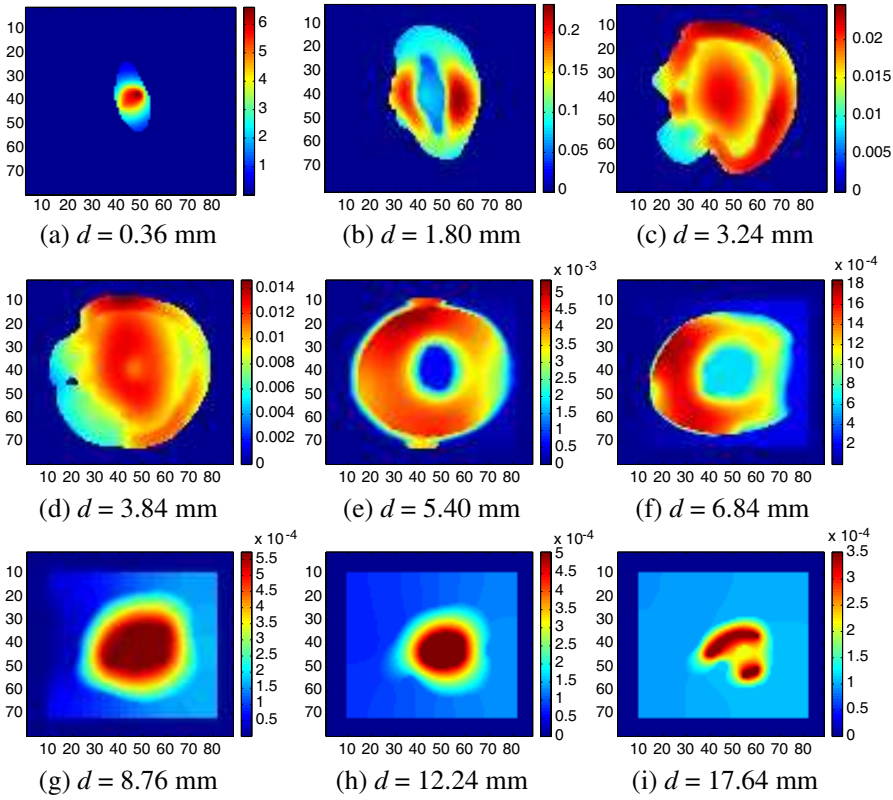

Figure 5. Electric potential (V) in nine transversal cross-sections through the tooth at a distance d from the 10 V electrode.

electrode (see Figure 6), the current density magnitude increases in the pulp up to 5 mA/m^2 at a distance of 5.40 mm from the top electrode. In these cross sections, the current in the enamel is very small. It is interesting to notice that proceeding down the tooth the current density magnitude values increase in the pulp (a few mA/m^2), as shown in Figures 6(g)–(i). The cross section (g) of Figure 6, which is located at the height of the bottom part of the ground electrode, is also interesting as it shows high values of the current density magnitude in the gum region close to the ground electrode.

Figure 7 shows the current density in three cross sections longitudinal to the tooth and parallel to the ground electrode for various distances from it. Figure 7(a) shows that the highest values of the current density magnitude are found in the bottom part of the ground electrode; this corresponds to Figure 6(g). Figure 7(b) shows

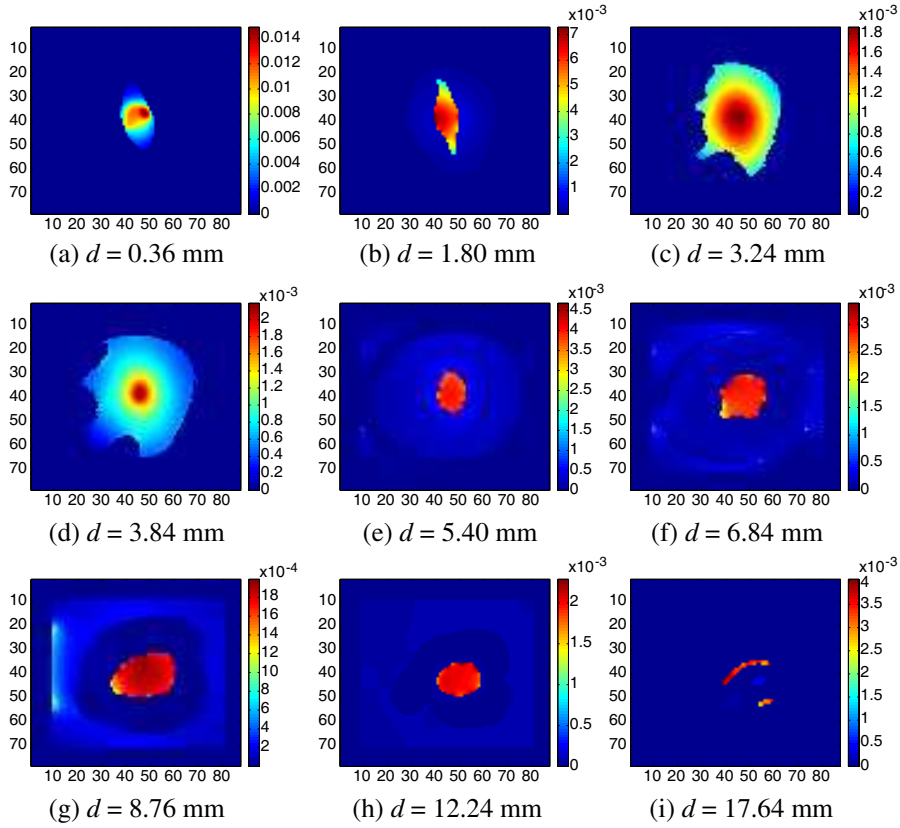

Figure 6. Current density (A/m^2) in nine transversal cross-sections through the tooth at a distance d from the 10 V electrode.

the current density magnitude distribution in a plane which cuts the top electrode; the current flows throughout all the pulp tissue from top to bottom. Figure 7(c) shows the current distribution in a cross section where only enamel and dentin tissues are present; it can be noticed that the highest values of the current density magnitude are found in the dentin and also in the top part of gum tissues.

Figure 8 shows the current density magnitude in three cross sections longitudinal to the tooth and perpendicular to the ground electrode. The distances are calculated from the reference x-z plane of the tooth model. The cross section (b) is normal to both electrodes; as Figure 7(b), it shows that the current flows in the pulp from top to bottom. The cross sections (a) and (c), which contain enamel and dentin tissues only, show that the highest values of the current density

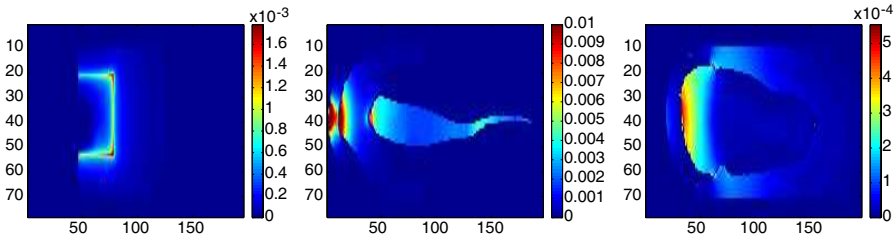

(a) $d = 0.12$ mm (b) $d = 4.2$ mm (c) $d = 6.84$ mm

Figure 7. Current density (A/m^2) in three longitudinal cross-sections through the tooth parallel to the ground electrode and at a distance d from it.

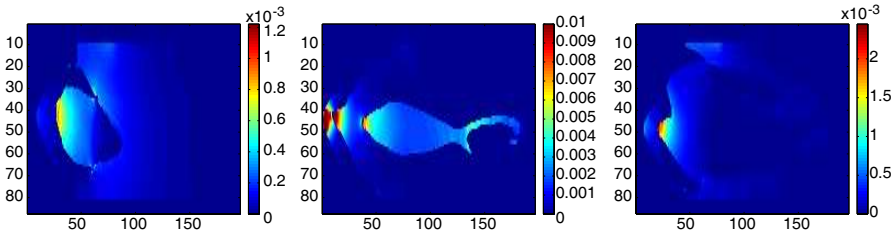

(a) $d = 0.84$ mm (b) $d = 3.36$ mm (c) $d = 5.4$ mm

Figure 8. Current density (A/m^2) in three longitudinal cross-sections through the tooth normal to the ground electrode at a distance d from the reference x-z plane.

magnitude are found in the dentin and also in the top part of gum tissues.

5. CONCLUSIONS

The calculation of the currents generated in dental tissues by the application of a dc voltage to the tooth is presented in this paper. In order to gain insight into the conduction mechanisms, a three-dimensional realistic voxel model of a human tooth was developed from a data set of digital images. The calculations employed a low-frequency numerical code (SPFD) that has already been validated in literature with respect to other numerical methods and proven accurate. The currents in the tooth model are calculated for an applied 10 V dc voltage between the electrodes. As it can be expected, the results show that the conduction mechanism in the tooth is influenced by the electrical conductivity of the tooth tissues. Indeed, it is interesting to notice that the currents, injected in the top of the tooth, flow

throughout the pulp and return to the ground electrode through the gum tissues. Although the resolution of the developed model can be deemed appropriate, increased resolutions can be adopted to refine the results.

The results of the current calculations are intended to be indicative only, as the position of the electrodes and their extension are arbitrary. Moreover, the tooth model can be further modified to include restorative materials with specified electrical properties [2].

ACKNOWLEDGMENT

The author is grateful to Brown and Herbranson Imaging, Inc., for providing the data set of digital images used in this paper. The author thanks Prof. U. Reggiani, of the same Department of the University of Bologna, Italy, for useful discussions. The work was supported in part by the grant Progetto Strategico di Ateneo IDeA, University of Bologna, Bologna, Italy.

REFERENCES

1. Pasquantonio, G., F. R. Tay, A. Mazzoni, P. Suppa, A. Ruggeri Jr., M. Falconi, R. Di Lenarda, and L. Breschi, "Electric device improves bonds of simplified etch-and-rinse adhesives," *Dental Materials*, Vol. 23, No. 4, 513–518, 2007.
2. Breschi, M., D. Fabiani, L. Sandrolini, M. Colonna, L. Sisti, M. Vannini, A. Mazzoni, A. Ruggeri, D. H. Pashley, and L. Breschi, "Electrical properties of resin monomers used in restorative dentistry," *Dental Materials*, Vol. 28, No. 9, 1024–1031, 2012.
3. Krizaj, D., J. Jan, and V. Valencic, "Modeling ac current conduction through a human tooth," *Bioelectromagnetics*, Vol. 25, No. 3, 185–195, 2004.
4. Dawson, T. W., J. De Moerloose, and M. A. Stuchly, "Comparison of magnetically induced elf fields in humans computed by FDTD and scalar potential FD codes," *Applied Computational Electromagnetics Society Journal*, Vol. 11, No. 3, 63–71, 1996.
5. Dawson, T. W. and M. A. Stuchly, "Analytic validation of a three-dimensional scalar-potential finite-difference code for low-frequency magnetic induction," *Applied Computational Electromagnetics Society Journal*, Vol. 11, No. 3, 72–81, 1996.
6. Dimbylow, P. J., "Induced current densities from low-frequency

magnetic fields in a 2 mm resolution, anatomically realistic model of the body," *Phys. Med. Biol.*, Vol. 43, 221–230, 1998.

7. Dawson, T. W. and M. A. Stuchly, "High-resolution organ dosimetry for human exposure to low-frequency magnetic fields," *IEEE Transactions on Magnetics*, Vol. 34, No. 3, 708–718, 1998.
8. Barchanski, A., M. Clemens, H. De Gersem, and T. Weiland, "Efficient calculation of current densities in the human body induced by arbitrarily shaped, low-frequency magnetic field sources," *J. Comput. Phys.*, Vol. 214, 81–95, May 2006.
9. Van Bladel, J., *Electromagnetic Fields*, McGraw-Hill, Inc., USA, 1964.
10. Dawson, T., M. Stuchly, K. Caputa, A. Sastre, R. Shepard, and R. Kavet, "Pacemaker interference and low-frequency electric induction in humans by external fields and electrodes," *IEEE Transactions on Biomedical Engineering*, Vol. 47, No. 9, 1211–1218, 2000.
11. Dawson, T., K. Caputa, M. Stuchly, and R. Kavet, "Electric fields in the human body resulting from 60-Hz contact currents," *IEEE Transactions on Biomedical Engineering*, Vol. 48, No. 9, 1020–1026, 2001.
12. Dawson, T. W., K. Caputa, M. A. Stuchly, and R. Kavet, "Pacemaker interference by 60-Hz contact currents," *IEEE Transactions on Biomedical Engineering*, Vol. 49, No. 8, 878–886, 2002.
13. Rao, A. K., K. Montgomery, W. P. Brown, and E. Herbranson, "3-D interactive atlas of human tooth anatomy," *CARS*, H. U. Lemke, M. W. Vannier, K. Inamura, A. G. Farman, K. Doi, and J. H. C. Reiber (eds.), 93–98, Elsevier, 2003.